

Pore formation in silicon by wet etching using micrometre-sized metal particles as catalysts

Chia-Lung Lee, Kazuya Tsujino, Yuji Kanda, Shigeru Ikeda and Michio Matsumura*

Received 10th October 2007, Accepted 19th December 2007

First published as an Advance Article on the web 21st January 2008

DOI: 10.1039/b715639a

Au, Pt, or Ag particles with particle sizes of *ca.* 1 μm were used as catalysts for boring pores in p-type Si(100) wafers by wet etching in aqueous solutions containing hydrofluoric acid and hydrogen peroxide. Boring speed was fastest when Pt particles were used as the catalyst. However, the sidewalls of the pores and the surface of the wafer were covered with a nanoporous silicon layer of *ca.* 500 nm in thickness, and the pore showed a tapered structure. When micrometre-sized Ag particles were used, no deep pores were formed because the particles were unstable in the solution. In contrast to Pt and Ag particles, Au particles bored straight pores under some conditions. However, the morphology of pores depended on the shape of the Au particles. Spherical Au particles formed straight pores, whereas non-spherical Au particles formed pores with spiral sidewalls. When Au particles formed aggregates consisting of a small number of particles (<10 particles), crooked pores tended to be formed. In contrast, when the aggregates were composed of a larger number of particles, straight pores were formed and the boring speed was faster than the pores formed with isolated Au particles.

Introduction

Deep straight pores formed in silicon (Si) have attracted attention for their applications in various fields such as membranes,^{1,2} trench capacitors,³ and through-wafer interconnects.^{4–6} Dry etching combined with photolithography has been commonly used for the fabrication of deep pores or trenches in Si.^{7,8} However, a major problem of this method is that it involves complicated processes for forming deep pores in Si, especially for making pores as deep as several tens of micrometres. Fabrication of pores in Si by this method is therefore costly, and the method is limited to small-scale production. Wet anisotropic etching in alkaline solution is another approach for making pores in Si. Although this method is attractive owing to its simplicity compared to dry etching, the realizable structures for desired applications are limited. Anodic etching, a process by which Si wafers are electrochemically anodized in solutions containing hydrofluoric acid (HF), is another attractive method because it enables the formation of deep pores.^{9,10} However, the complexity of pretreatment that is required for making the patterned structure impedes the application of this method to mass production.

Metal-assisted etching has been studied as a novel method for production of a porous structure in Si. In this method, thin metal films or particles loaded on Si wafers are used as catalysts for etching of Si in aqueous solutions containing HF and oxidants such as H_2O_2 ,^{2,11–16} $\text{Fe}(\text{NO}_3)_3$,¹⁷ $\text{K}_2\text{Cr}_2\text{O}_7$ ¹⁸ and O_2 ¹⁹ without the need for external electrical power. Because of the simplicity of this method compared to the common techniques described above, the method is promising for application to mass production if efficient control of the geometrical structure is achieved.

We previously reported that cylindrical pores of several tens of nanometres in diameters were formed in Si preferentially in the <100> direction by wet etching in an aqueous solution containing HF and H_2O_2 using Ag particles as catalysts.¹⁴ The Ag particles were loaded on the Si surface before the etching. During the etching, the Ag particles sank into the bulk of Si and formed pores.^{14,16} When Pt particles with granular surfaces were used instead of the Ag particles, helical pores were formed.¹⁵ Zhu *et al.*^{13,17} reported the formation of straight Si nanowire arrays perpendicular to the Si wafer by a method similar to ours using densely deposited Ag particles as catalysts and H_2O_2 or $\text{Fe}(\text{NO}_3)_3$ as oxidant.

In order to apply the pores to through-wafer interconnects, the pore diameter should be larger than 1 μm .^{4–6} Hence, our research interest has been focused on the fabrication of pores with diameters larger than 1 μm by applying the metal-assisted etching technique. Here, we report the usefulness of micrometre-sized metal particles as catalysts for the fabrication of such large pores. We also report the effects of shapes, states of aggregation, and kind of metal particles used as the catalysts on the morphology of the pores formed.

Experimental

The Si wafer used in the present study was p-type Si(100) (boron-doped, 7–13 Ωcm). The wafer was 625 μm in thickness, and one of the faces was mirror-polished. The wafer was cut into 20 \times 20 mm^2 pieces and used as test samples. Two kinds of micrometre-sized Au particles were used: spherical Au particles purchased from Tokuriki Chemical Research and non-spherical particles obtained from Aldrich. Pt and Ag microspheres were obtained from Ishifuku Metal Industry and Mitsui Mining & Smelting, respectively. Laboratory-grade ultra-pure water (UPW) with a resistivity of 18.2 $\text{M}\Omega\text{cm}$ was prepared using a Milli-Q pure water

Research Center for Solar Energy Chemistry, Osaka University, 1-3 Machikaneyama, Toyonaka, 560-8531, Japan. E-mail: matsu@chem.es.osaka-u.ac.jp; Fax: +81-6-6850-6699; Tel: +81-6-6850-6695

system (YAMATO-Millipore). Other chemicals were used as received.

Before the pore formation, the Si sample was cleaned by immersing it in a sulfuric acid–hydrogen peroxide mixture (97% H_2SO_4 –30% H_2O_2 , 4 : 1 v/v) for 10 min, in 1% HF for 1 min, and in UPW for 10 min for rinsing. Then it was again immersed in a sulfuric acid–hydrogen peroxide mixture for 10 min, rinsed with UPW for 10 min, and dried by air blowing. The surface of the sample was hydrophilic. On the mirror-polished face of the sample, the dispersion of metal particles suspended in water or isopropyl alcohol was placed dropwise and spin-cast with a Mikasa 1H-D7 spincoater at a speed of 3000 rpm. Then the Si sample loaded with the metal particles was immersed in an aqueous solution containing HF and H_2O_2 for etching for certain periods. After the etching treatment, the Si sample was rinsed successively with UPW for 10 sec, ethanol for 3 min, and pentane for 3 min, and dried in air. Morphologies of the metal particles and pores formed in Si samples were observed using a Hitachi S-5000 scanning electron microscope (SEM). Cross-sectional views of samples were obtained for the surfaces exposed by mechanically cleaving the sample. Pores were preferentially formed in the $\langle 100 \rangle$ direction,¹⁴ especially when spherical particles were used as the catalyst. When a sample with pores that developed in the $\langle 100 \rangle$ direction at a high density was cleaved mechanically, the sample tended to be cleaved along the pores. However, the observation of cleaved pores was rather difficult when the density of the pores was low or the pores were crooked. In such samples, cross sections of the pores could be observed.

Results and discussion

Pore formation using spherical and non-spherical Au particles as catalysts

Fig. 1a shows a typical SEM image of spherical Au particles loaded on a Si(100) surface by the spin-coating method. The Au particles had diameters of about 0.5–1.5 μm . They were randomly distributed: there were isolated particles and aggregated particles. Other metal particles employed here also showed similar distributions when loaded on Si surfaces. When a Si sample loaded with Au particles was immersed in an aqueous solution containing HF (2.6 mol dm^{-3}) and H_2O_2 (8.1 mol dm^{-3}) for 1 h, Au particles disappeared completely, and micrometre-sized pores were generated, as shown in Fig. 1b. The density of pores formed was almost equivalent to that of Au particles loaded, while the sizes of these pores were larger than that of Au particles. Corresponding cross-sectional SEM images revealed the presence of the Au particles at the bottoms of pores, shown in Fig. 2. Hence, like the formation of deep nanoholes with Ag nanoparticles,^{14,16} micrometre-sized pores were found to be formed with Au particles, which sank into the Si as the pores were formed. It is noted that, when a Si(111) wafer was employed, the deep pores were oriented at about 55° from the surface (data not shown), indicating that the pores grew preferentially in the $\langle 100 \rangle$ direction. This result is also in agreement with the pores formed by Ag nanoparticles.^{14,16}

Previous studies have shown that the pore formation is initiated by the reduction of H_2O_2 , as represented by eqn (1).^{14,16}

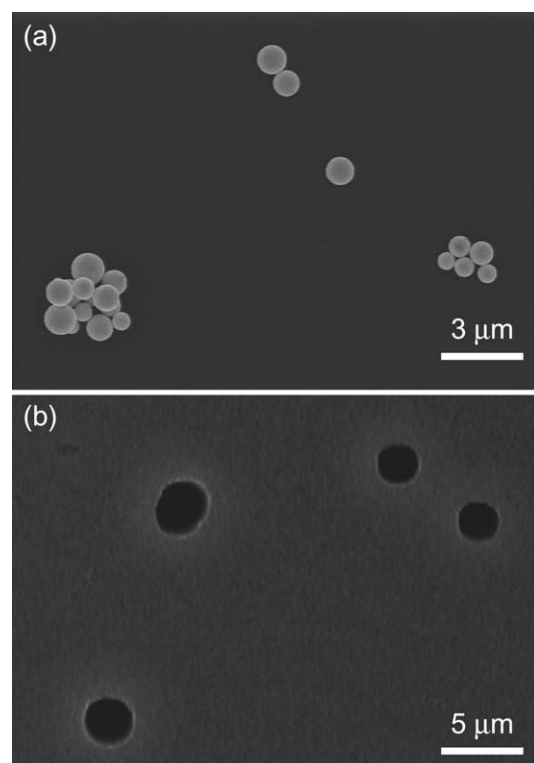
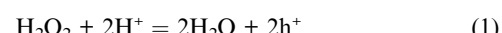
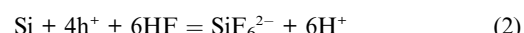


Fig. 1 SEM images of (a) a Si(100) surface loaded with spherical Au particles and (b) the surface after immersion in an aqueous solution containing 2.6 mol dm^{-3} HF and 8.1 mol dm^{-3} H_2O_2 for 1 h.



Owing to the low catalytic ability of the Si surface for the reaction, the etching of Si is slow in a HF– H_2O_2 solution. However, the reaction is catalyzed by Au, Pt or Ag particles. Since these metal particles donate electrons to H_2O_2 and accept electrons from Si, positive holes are generated in Si. The positive holes injected into Si induce oxidative dissolution of Si in a solution containing HF, which is represented by eqn (2).



Since the oxidative dissolution occurs preferentially near the metal–Si interface, micrometre-sized pores are formed. As typically shown in Fig. 2a, the pores formed with the isolated Au particles were mostly linear and oriented in the $\langle 100 \rangle$ direction. The preferential boring in the $\langle 100 \rangle$ direction is attributed to the chemical instability of the (100) face. It has been reported that the oxidative dissolution of Si in HF solution, either caused by chemical oxidation or electrochemical oxidation, is accompanied by the formation of a nanoporous Si layer on the surface.¹¹ The formation of the nanoporous Si layer is enhanced under the condition in which a large number of positive holes are injected into Si. Such nanoporous Si layers were observed in our samples in the magnified SEM images of pore sidewalls and top surfaces of samples after the treatment. The thickness was about 100 nm.

In contrast to the pores formed with isolated Au particles, those formed with Au deposits consisting of a few Au particles were often crooked, as seen in Fig. 2b. A probable explanation

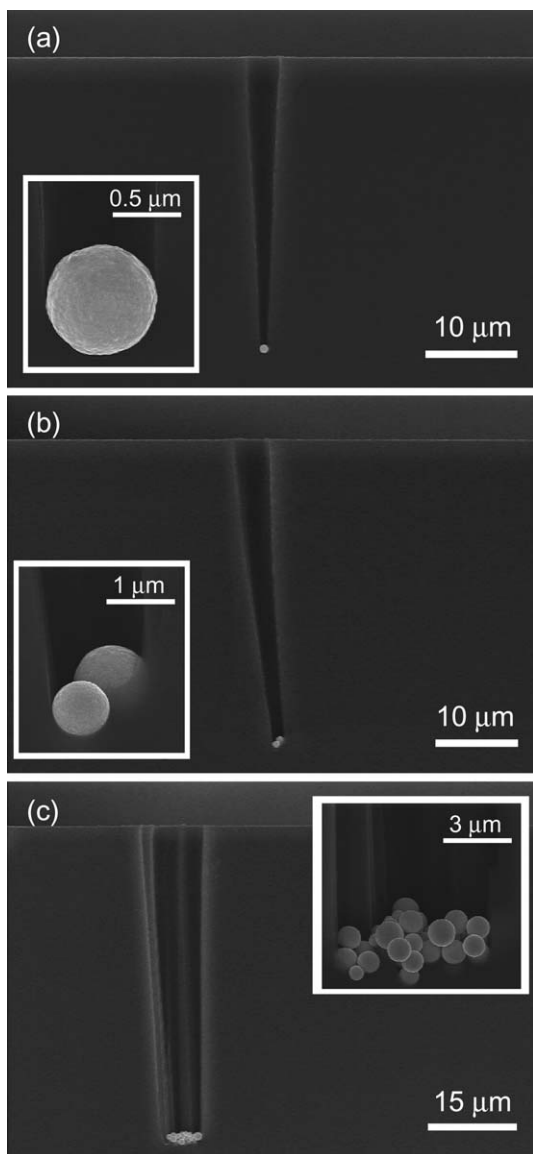


Fig. 2 Cross-sectional SEM images of the pores bored in a Si(100) sample with (a) a single spherical Au particle, (b) an aggregate composed of two Au particles, and (c) an aggregate composed of a large number of Au particles after etching in an aqueous solution containing 2.6 mol dm^{-3} HF and 8.1 mol dm^{-3} H_2O_2 for 1 h. Insets show their corresponding enlarged images of the bottom parts of pores.

for the results is that the irregular geometry of the Au–Si interface on the deposit induced different local etching rates on the deposit, resulting in the deviation of the pore growth direction from the $\langle 100 \rangle$ direction. However, when the deposit consisted of a larger number of Au particles, especially more than 10 particles, the pores again grew in the $\langle 100 \rangle$ direction, as shown in Fig. 2c. In this case, the local difference in the etching rate at the Si–Au interface was probably averaged and, as a result, straight pores were formed. This result is similar to the growth of Si nanowires using densely deposited nano-sized Ag particles.^{13,17} Our finding indicates that such an averaging effect occurs even with deposits consisting of only 10 or more particles.

As seen in Fig. 2a and 2c, the straight pore formed with aggregated Au particles is almost twice as deep as that formed with an

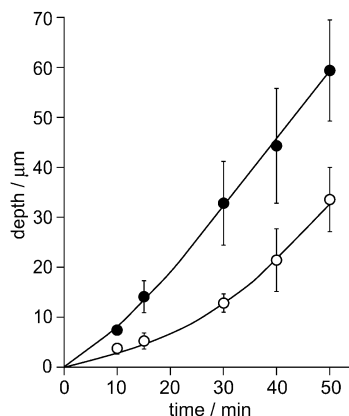


Fig. 3 Depth of pores formed with isolated Au particles (○) and Au aggregates consisting of more than 10 particles (●) vs. etching time. Each point shows the average for about 10 pores and the bar represents the standard deviation.

isolated Au particle, both being formed by a 1 h treatment. Fig. 3 shows the depths of pores generated with isolated Au particles and Au aggregates consisting of more than 10 particles as a function of the treatment time. The faster boring speed for the aggregated Au particles is attributable to the larger surface area of the 3-dimensionally aggregated structure of the Au particles. This structure allows the reduction of H_2O_2 in a larger amount per unit area of the cross section of the pore and an increase in the number of positive holes injected into Si. The efficient diffusion of HF, H_2O_2 and SiF_6^{2-} in the large pores bored by them may also contribute to the rapid growth of pores. The relatively slow boring speed in the initial period, as seen in Fig. 3, suggests that the Au particles deposited on the Si surface by spin-casting do not make good physical contact with Si. In addition, when the particles are deposited on Si with a flat surface, the contact area must be small. However, after the particles start sinking into Si, the contact area between Au and Si increases, leading to the increased boring speed.

Another feature of the pores seen in Fig. 2 is that the widths are larger at the upper part of the pores. This phenomenon suggests that part of the positive holes diffused from the bottom of the pores, where Au particles existed, to the sidewalls of the Si sample and formed nanoporous Si layers. Since the nanoporous Si gradually dissolves into the HF solution,^{20–22} Si is etched more at places where the surface is in contact with the HF solution for a longer time. This results in the formation of pores with conical shapes, as shown in Fig. 2a. The widening of the pores is therefore related to the ability of positive-hole injection from the catalytic particles: this increases in the order of Ag, Au and Pt (see below).

The pore bored with the Au particle can penetrate through a 625 μm -thick wafer after treatment for 18 h, as shown in Fig. 4a. These through-wafer pores were seen as bright spots under an optical microscope by illuminating the sample from the rear side. When the Au particles reached the back surface, they shifted to some extent along the plane, and started to move back toward the front surface (Fig. 4b). Since the backward movement may pose a problem for its application to through-wafer interconnects, we are now studying a method to prevent the backward movement of the particles. Interestingly, aggregates

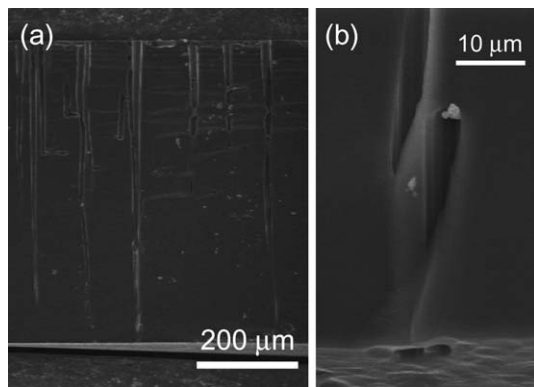


Fig. 4 (a) Cross-sectional SEM images of a Si(100) sample loaded with spherical Au particles after etching in an aqueous solution containing 2.6 mol dm^{-3} HF and 8.1 mol dm^{-3} H_2O_2 for 18 h, and (b) a cross-sectional SEM image of the bottom part of the sample shown in panel (a).

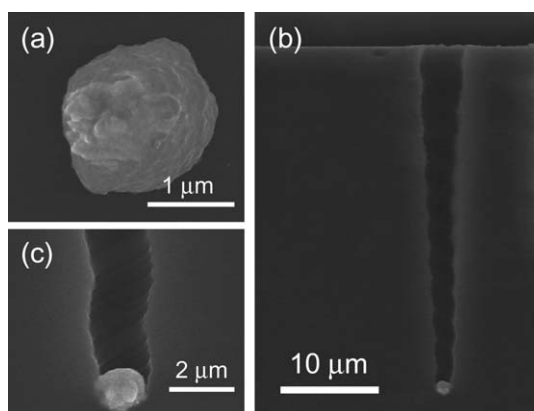


Fig. 5 (a) SEM image of a non-spherical Au particle loaded on a Si(100) surface. (b) Cross-sectional SEM image of a non-spherical Au-loaded Si(100) sample after etching in an aqueous solution containing 2.6 mol dm^{-3} HF and 8.1 mol dm^{-3} H_2O_2 for 1 h. (c) Enlarged image of the bottom part of the pore shown in panel (b).

made of a very large number of particles did not move along the plane and stayed at the place where they reached (data not shown).

So far, we have explained the results obtained with spherical Au particles. When we used non-spherical Au particles, *i.e.*, the particle distorted from a sphere (Fig. 5a), the pores formed showed different morphologies. Fig. 5b shows a representative cross-sectional SEM image of the pore formed with the non-spherical Au particles. A pore grew perpendicularly to the sample surface to a depth of about 33 μm in 1 h. The depth was nearly the same as that of the pore generated with a spherical Au particle of nearly the same size. A significant difference between these pores is that the sidewall of the pore generated with a non-spherical Au particle was somewhat spiraled and had many parallel stripes, as shown in Fig. 5c. This structure suggests that the Au particle rotated as it sank into Si. The irregular surface morphology of the Au particle is likely to induce spatial variation in the supply of positive holes to Si, leading to the different etching rate on a particle. This provides the driving force to rotate the Au particle. This phenomenon is similar to

the process by which helical pores were formed with irregularly shaped Pt nanoparticles,¹⁵ in which Pt rotated around axes as they sank into Si. It should be noted that when the non-spherical Au particles formed an aggregate consisting of more than 10 particles, the pore became straight, as were the pores formed by an aggregate of spherical Au particles.

Pore formation using spherical Pt or Ag particles as catalysts

In addition to the Au particles, we used Pt and Ag particles as catalysts. Their morphologies were similar to the spherical Au particles shown in the preceding section. When we used Pt particles, straight pores with diameters of several micrometres were easily obtained, as shown in Fig. 6. The Pt particles showed much stronger catalytic activity for making the pores, and, hence, we lowered the concentration of H_2O_2 in the etching solution to 0.18 mol dm^{-3} , but we increased the concentration of HF from 2.6 mol dm^{-3} to 5.3 mol dm^{-3} because the oxidation rate was increased. The pores formed after 1 h treatment using Pt particles were still about 1.4 times deeper than those formed after 1 h treatment using Au particles in the etching solution containing 8.1 mol dm^{-3} H_2O_2 and 2.6 mol dm^{-3} HF. Another feature of the pores made with Pt particles is that the upper part of the pores is broadened remarkably, forming conical-shaped pores. In addition, the SEM images show that a thick nano-porous Si layer (*ca.* 500 nm) was formed over the sidewalls of the conical shaped pores and the sample surface. All of these results indicate that Pt particles have strong catalytic activity for the injection of positive holes into Si because Pt has stronger catalytic activity for the reduction of H_2O_2 .²³ The enhanced supply of positive holes into Si leads to the increased boring speed, broadening of the pore width, and growth of the nanoporous Si layer, as discussed above. Hence, the fast etching of Si using Pt as a catalyst is attributed to the effective formation of positive holes at the Pt–solution interface. The ease of transport of positive holes across the Pt–Si interface may also contribute to the strong catalytic activity.

When spherical Ag particles of about 0.5–1.5 μm in diameter were used as the catalyst, very few deep pores were bored, but pits of several μm in depth were formed, as shown in Fig. 7a. The treatment was carried out under the same conditions as those used for the treatment with Pt particles in an aqueous

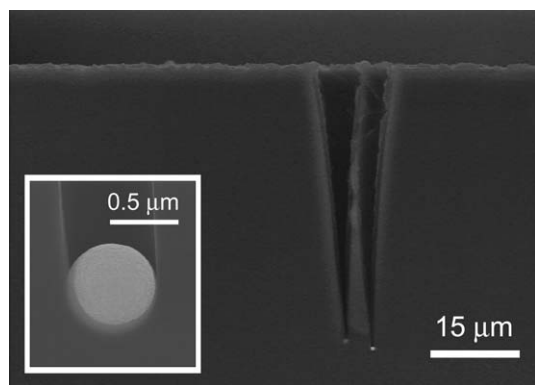


Fig. 6 Cross-sectional SEM image of a Si(100) sample loaded with spherical Pt particles after etching in an aqueous solution containing 5.3 mol dm^{-3} HF and 0.18 mol dm^{-3} H_2O_2 for 1 h. Inset shows a corresponding enlarged image of the bottom part of the pore.

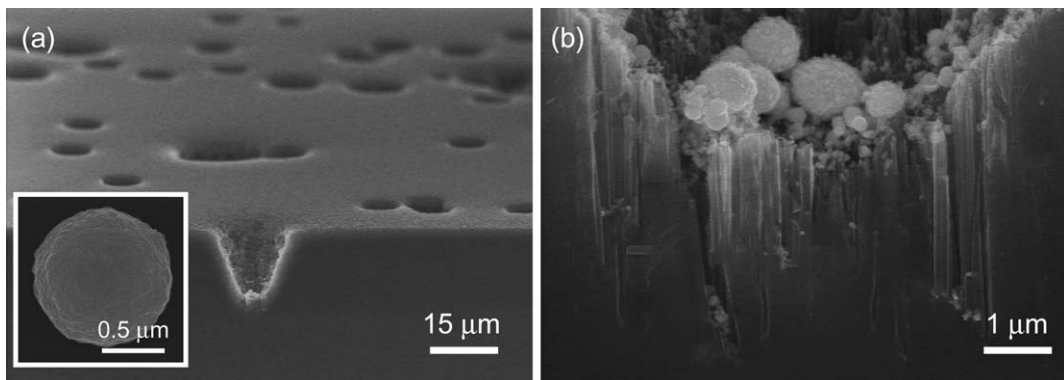


Fig. 7 (a) Surface and cross-sectional SEM image of a Si(100) sample loaded with spherical Ag particles after etching in an aqueous solution containing 5.3 mol dm^{-3} HF and 0.18 mol dm^{-3} H_2O_2 for 20 min. (b) Enlarged image of one of the pits shown in panel (a). Inset of panel (a) shows an SEM image of an Ag particle before being used as the catalyst.

solution containing HF (5.3 mol dm^{-3}) and H_2O_2 (0.18 mol dm^{-3}) for 20 min. The pH of the solution was about 0.3. A magnified image of the pit (Fig. 7b) shows characteristic features that were not seen when Au or Pt particles were used. These features are as follows: (1) many particles of different sizes ranging from *ca.* 1 μm , which is the size of the original particle, down to *ca.* 0.05 μm , exist at the bottom of the pit; (2) each of the particles has an irregular and granular structure, in contrast to the original Ag particle; (3) several nanometre-sized straight pores of *ca.* 4 μm in depth were formed, and (4) tiny particles are seen at the bottom of the nanometre-sized pores. These results suggest that the micrometre-sized Ag particles have weak catalytic activity to bore Si in marked contrast to those of the nanometre-sized Ag particles, which are effective for pore formation.¹⁴ The nanometre-sized pores are attributed to those formed by nanometre-sized Ag particles that were re-deposited from Ag ions, which had been dissolved from the micrometre-sized Ag particles.

The uniqueness of the properties of micrometre-sized Ag particles as a catalyst for boring pores in Si is correlated with its electrochemical properties. Since Ag has a relatively negative redox potential (Ag^+/Ag^0 , 0.80 V vs. NHE) compared to those of Pt ($\text{Pt}^{2+}/\text{Pt}^0$, 1.19 V vs. NHE) and Au ($\text{Au}^{3+}/\text{Au}^0$, 1.50 V vs. NHE), Ag particles are easily oxidized and dissolved into the solution containing H_2O_2 , which has a redox potential of 1.72 V vs. NHE in a solution at pH 0.3. However, when they are in contact with Si, the dissolution of Ag particles can be suppressed by the supply of electrons from Si (or supply of positive holes from Ag to Si) through the Si–Ag interface, resulting in oxidative dissolution of Si instead of Ag. This process takes place easily, since the flat band potential of p-type Si is located at about 0.38 V vs. NHE,²⁴ which is more negative than the redox potential of silver. This leads to boring of cylindrical nanoholes by Ag nanoparticles.^{14,16} However, in the case of micrometre-sized Ag particles, the lowered ratio of the Ag–Si contact area to the surface area of an Ag particle leads to undersupply of electrons from Si to Ag particles. As a result, the electrochemical potential (or the Fermi level) of Ag particles shifts to a level that is sufficiently positive to dissolve Ag into the solution. The Ag^+ ions in the solution can be reduced and re-deposited as tiny particles on Si surfaces concomitantly with the oxidative dissolution of Si

in HF-containing solution because Si is more likely to be oxidized than Ag.^{25,26} Hence, the tiny particles seen in Fig. 6 are attributed to Ag particles that were re-deposited from Ag^+ ions, which had been dissolved from the micrometre-sized Ag particles. Since nanometre-sized Ag particles are good catalysts for making pores in Si, the tiny pores formed from the bottom of the pits are attributed to those formed by the re-deposited Ag particles. These Ag particles are deposited near the bottom of the pits because the deposition occurs preferentially in the region where the concentration of Ag^+ ions is high.

Conclusion

We have studied the usefulness of micrometre-sized metal particles as catalysts for the fabrication of micrometre-sized pores in Si(100) wafers by wet etching. The formation of pores includes various elementary steps, *e.g.*, reduction of H_2O_2 on metal catalysts, injection of electrons from Si to metal catalysts, and oxidative dissolution of Si with positive holes and HF. The pore formation and the morphologies of the pores are affected not only by the kind of metal particles used as catalyst but also by the size and shape of the particles. Among the catalysts used in the present study, we found that spherical Au microspheres are promising candidates for making straight pores with micrometre-sized diameters. They can be used as isolated particles or in the state of relatively large aggregates (>10 particles).

Acknowledgements

One of the authors (K.T.) expresses his special thanks for financial support from Research Fellowships of the Japan Society for the Promotion of Science for Young Scientists. This work was supported by a Grant-in-Aid for Scientific Research on Fundamental Research and by a Grant-in-Aid for Scientific Research on Priority Areas (No. 458), each from the Ministry of Education, Culture, Sports, Science and Technology of the Japanese Government.

References

- 1 S. E. Létant, B. R. Hart, A. W. van Buuren and L. J. Terminello, *Nat. Mater.*, 2003, **2**, 391.

- 2 S. Cruz, A. Hönig-d'Orville and J. Müller, *J. Electrochem. Soc.*, 2005, **152**, C418.
- 3 S. J. Lin, C. S. Lai, S. H. Liao, C. Y. Lee, P. I. Lee, S. M. Chiang and M. W. Liang, *IEEE Trans. Semicond. Manuf.*, 2005, **18**, 644.
- 4 K. Takahashi, H. Terao, Y. Tomita, Y. Yamaji, M. Hoshino, T. Sato, T. Morifushi, M. Sunohara and M. Bonkohara, *Jpn. J. Appl. Phys., Part 1*, 2001, **40**, 3032.
- 5 L. W. Schaper, S. L. Burkett, S. Spiesshoefer, G. V. Vangara, Z. Rahman and S. Polamreddy, *IEEE Trans. Adv. Packag.*, 2005, **28**, 356.
- 6 M. Koyanagi, T. Nakamura, Y. Yamada, H. Kikuchi, T. Fukushima, T. Tanaka and H. Kurino, *IEEE Trans. Electron Devices*, 2006, **53**, 2799.
- 7 S. Panda, R. Ranade and G. S. Mathad, *J. Electrochem. Soc.*, 2003, **150**, G612.
- 8 I. W. Rangelow, *J. Vac. Sci. Technol., A*, 2003, **21**, 1550.
- 9 V. Lehmann, *J. Electrochem. Soc.*, 1993, **140**, 2836.
- 10 V. Lehmann and S. Rönnebeck, *J. Electrochem. Soc.*, 1999, **146**, 2968.
- 11 X. Li and P. W. Bohn, *Appl. Phys. Lett.*, 2000, **77**, 2572.
- 12 X. H. Xia, C. M. A. Ashruf, P. J. French and J. J. Kelly, *Chem. Mater.*, 2000, **12**, 1671.
- 13 H. Fang, Y. Wu, J. Zhao and J. Zhu, *Nanotechnology*, 2006, **17**, 3768.
- 14 K. Tsujino and M. Matsumura, *Adv. Mater.*, 2005, **17**, 1045.
- 15 K. Tsujino and M. Matsumura, *Electrochem. Solid-State Lett.*, 2005, **8**, C193.
- 16 K. Tsujino and M. Matsumura, *Electrochim. Acta*, 2007, **53**, 28.
- 17 K. Q. Peng, J. J. Hu, Y. J. Yan, Y. Wu, H. Fang, Y. Xu, S. T. Lee and J. Zhu, *Adv. Funct. Mater.*, 2006, **16**, 387.
- 18 T. Hadjersi, N. Gabouze, N. Yamamoto, C. Benazzouz and H. Cheraga, *Vacuum*, 2005, **80**, 366.
- 19 S. Yae, Y. Kawamoto, H. Tanaka, N. Fukumuro and H. Matsuda, *Electrochim. Commun.*, 2003, **5**, 632.
- 20 H. Unno, K. Imai and S. Muramoto, *J. Electrochem. Soc.*, 1987, **134**, 645.
- 21 A. Pascual, J. F. Fernández, C. R. Sánchez, S. Manotas and F. Agulló-Rueda, *J. Porous Mater.*, 2002, **9**, 57.
- 22 D. Hamm, S. Sakka and Y. H. Ogata, *Electrochemistry*, 2003, **71**, 853.
- 23 R. D. O'Neill, S.-C. Chang, J. P. Lowry and C. J. McNeil, *Biosens. Bioelectron.*, 2004, **19**, 1521.
- 24 S. Ottow, G. S. Popkirov and H. Föll, *J. Electroanal. Chem.*, 1998, **455**, 29.
- 25 M. V. ten Kortenaar, J. J. M. de Goeij, Z. I. Kolar, G. Frens, P. J. Lusse, M. R. Zuiddam and E. van der Drift, *J. Electrochem. Soc.*, 2001, **148**, C28.
- 26 F. M. Liu and M. Green, *J. Mater. Chem.*, 2004, **14**, 1526.